Doping engineering to increase the material yield during crystallization of B and P compensated silicon

Maxime Forster, Erwann Fourmond, Roland Einhaus, Hubert Lauvray, Jed Kraiem, Mustapha Lemiti

DOPING ENGINEERING TO INCREASE THE MATERIAL YIELD DURING CRYSTALLIZATION OF B AND P COMPENSATED SILICON

Maxime Forster[1,2*], Erwann Fourmond[2], Roland Einhaus[1], Hubert Lauvray[1], Jed Kraiem[1], Mustapha Lemiti[2]
[1] APOLLON SOLAR, 23 rue Claudius Collonge, 69002, Lyon, France
[2] INSA de LYON, INL, 7 av. J. Capelle, 69621 VILLEURBANNE CEDEX
*Corresponding author : E-mail: forster@apollonsolar.com

ABSTRACT: In this paper, we investigate gallium co-doping during crystallization of boron and phosphorus compensated Si. It is shown that the addition of gallium yields a fully p-type ingot with high resistivity despite high B and P contents in the silicon melt. Segregation of doping impurities is consistent with theory. Minority carrier lifetime and majority carrier mobility measurements indicate that this material is suitable for the realization of solar cells with comparable efficiencies to standard material. Significant light-induced degradation of minority carrier lifetime is however revealed to occur in this material as in standard boron-doped silicon.

1 INTRODUCTION

In the drive to reduce the cost of solar energy, one promising path is the use of low cost Si feedstock, or Upgraded Metallurgical Grade Si (UMG-Si), obtained by simplified purification processes [1]. This kind of material was recently shown to offer a great potential in terms of cell performances when it is sufficiently purified [2]. However, it usually contains more impurities than EG (Electronic Grade) silicon that may harm the photovoltaic performance of this material. Among them, B and P are the most difficult to remove through metallurgical processes and may thus remain in concentration up to 10ppmw after purification. Such a Si, containing both B and P in significant concentration is designated as compensated Si and shows modified electrical properties compared to uncompensated B-doped Si. These electrical properties (resistivity, minority carrier lifetime) depend critically on the net doping N_A-N_D. Previous results [3] have shown the minority carrier lifetime to be higher and thus solar cells to be more efficient at high compensation levels (C_l), i.e. for low net doping, (or high resistivity). In addition, a lower net doping seems to lead to a reduction of the light-induced degradation observed in B-doped and oxygen contaminated Si [4].

However, because of the lower segregation coefficient of phosphorus (0.35) compared to that of boron (0.8), the net doping is not uniform along the ingot height and inversion of Si polarity, from p- to n-type may occur during crystallization (**Fig.1**), reducing the material yield for standard industrial solar cell fabrication. Simulations [5] using Scheil's law for dopant distribution and simple models for calculating carrier mobility show that requiring a minimum resistivity of 0.5Ω.cm and an ingot yield of at least 90% compels the use of Si feedstock containing less than 0.45ppmw of B and 1.0ppmw of P. Gallium co-doping has recently been proposed [6-8] as a potential solution to control the net doping along the ingot height even when using Si containing large quantities of B and P. It relies on the low segregation coefficient of Ga which enables the increased P concentration, in relation to B, to be counterbalanced during crystal growth (**Fig.2**). It is thus possible to obtain low net doping and p-type Si along the full ingot height. In this work, mono- and multi-crystalline ingots were grown using intrinsic solar grade polysilicon to which was voluntarily added known concentrations of B, P and Ga before crystallization. The resulting electrical properties were studied and correlated to the doping impurities vertical distribution along the ingot height.

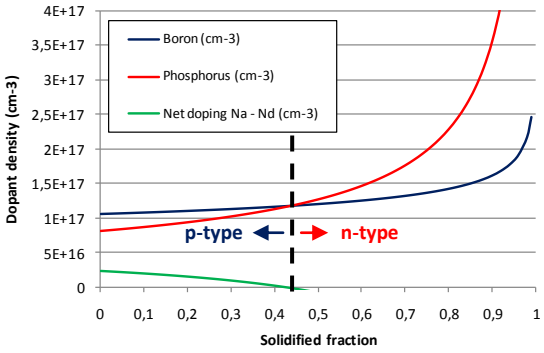

Figure 1: B, P and net doping distribution calculated with Scheil's law along the height of an ingot which would be crystallized with Si containing 1ppmw of B and 5ppmw of P.

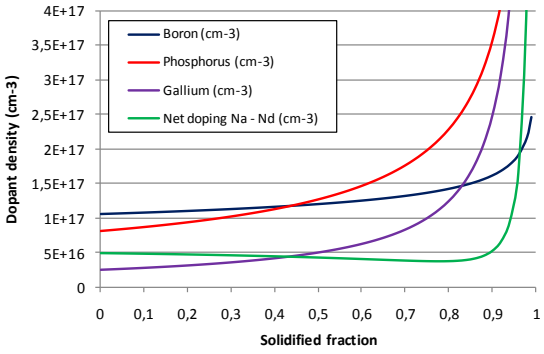

Figure 2: B, P, Ga and net doping distribution calculated with Scheil's law along the height of an ingot which would be crystallized with Si containing 1ppmw of B, 5ppmw of P and with the addition of 150ppmw of Ga.

2 EXPERIMENTAL DETAILS

2.1 Crystallization and wafering

For this study, two 15kg mono-crystalline and one 35kg multi-crystalline ingots were grown. The mono-crystalline ingots Cz#1 and Cz#2 were <100> oriented Si crystals of about 160mm in diameter grown with the Cz method at Siltronix. The multi-crystalline ingot Mc#1 was grown in a casting furnace developed by Cyberstar and Apollon Solar [10,11]. Each ingot was made with intrinsic solar grade poly-Si to which known

concentrations of B, P and Ga were added (**Table 1**). The concentrations of B and P added in ingot Cz#1 correspond to an UMG-Si from which B has been efficiently removed by purification but which still contains high amounts of P. The B and P concentrations in ingots Cz#2 and Mc#1 correspond to a less purified UMG-Si. In each case, the Ga concentration to be added was calculated using the Scheil's law in order to obtain a fully p-type ingot and relatively high resistivity. B and P were introduced through highly doped Si wafers in which the doping impurity concentration was evaluated by means of four-point probe resistivity measurements correlated to the Irvin curves. Ga was introduced in the form of high purity Ga pellets. All the dopant sources were precisely weighed and put into the crucible together with the Si feedstock before melting. Ingot Cz#1 was then shaped into a 125x125mm² pseudo-square brick and sliced into 240µm thick wafers which were KOH etched to remove saw damage.

Table 1: Initial dopant concentrations added into the crucible before fusion for the three studied ingots.

Ingot	B_0 (cm-3)	P_0 (cm-3)	Ga_0 (cm-3)
Cz#1	$2.7x10^{16}$	$1.8x10^{17}$	$5.8x10^{18}$
Cz#2	$2.1x10^{17}$	$3.2x10^{17}$	$3.6x10^{18}$
Mc#1	$2.1x10^{17}$	$3.2x10^{17}$	$3.6x10^{18}$

2.2 Characterization

Resistivity was measured by Eddy currents at various heights along the length of each ingot in order to evaluate the impact of Ga co-doping.

Additional characterizations were held on ingot Cz#1: SIMS analyses on wafers from different ingot heights to determine the vertical distribution of doping impurities. Four-point probe resistivity and Hall effect measurements were performed to study the electrical activation of dopants. Minority carrier lifetimes were measured by QSSPC after chemical polishing and surfaces passivation by Si-rich SiNx:H layer deposition by PECVD, which was shown to ensure an optimum surface passivation [12]. Lifetime measurements were done after a six day light soaking under a 70 mW/cm² halogen lamp for full B-O complexes activation, and after an annealing step during 20 min at 210°C in the dark.

3 RESULTS

3.1 Resistivity

Measured resistivities are shown in Figure 3. For each ingot, the Si is p-type and the resistivity higher than 0.5Ω.cm along the full ingot height, despite high concentrations of B and P. Moreover, one can see that the resistivity is comprised in a very narrow range (0.5 to 1.2Ω.cm) along the full length of ingots Cz#2 and Mc#1. This indicates that Ga co-doping was efficient for:

(1) Avoiding Si to turn n-type. Indeed, using the Scheil's law, one can expect from B and P initial concentrations that the entire ingot Cz1 would be n-type and that a type inversion should occur at around 60% of the heights of ingot Cz2 and Mc1 if no Ga had been added before crystallization.

(2) Maintaining a relatively low net doping since the resistivity is kept higher than 0.5Ω.cm.

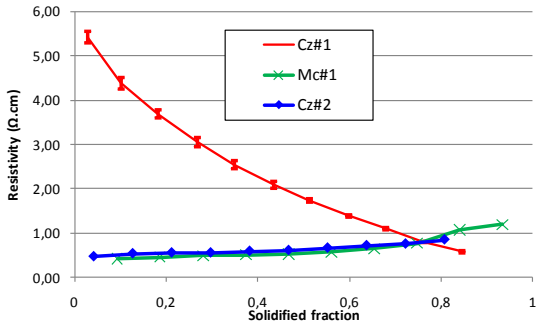

Figure 3: Resistivity measured at different heights along the length of ingots Cz#1, Cz#2 and Mc#1.

3.2 SIMS analyses

SIMS analyses (**Fig.4**) confirm that the p-type resistivity is to be attributed to the addition of Ga. Indeed, one can observe that the P concentration exceeds that of B over the entire ingot height, suggesting that without Ga co-doping, the ingot would be fully n-type.

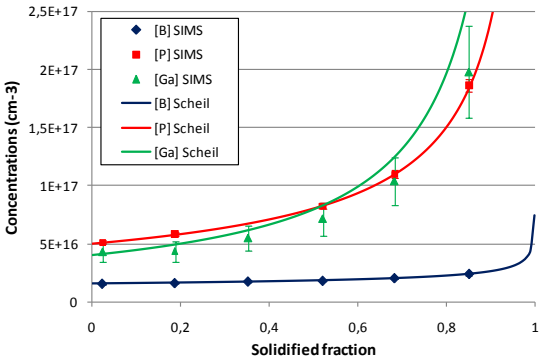

Figure 4: B, P and Ga concentrations measured by SIMS at various heights of ingot Cz1. The solid lines are the fits to Scheil's equation.

$$C_S = k_{eff} \cdot C_0 \cdot (1 - f_S)^{k_{eff}-1} \qquad \textbf{Eq. 1}$$

The effective segregation coefficients k_{eff} of B and P can be extracted by fitting Scheil's equation (**Eq.1**) to the measured concentration of these two impurities. The extracted segregation coefficients equal 0.77 and 0.32 respectively for B and P, these values being in good agreement with theoretical values (0.8 for B and 0.35 for P [13]). SIMS analyses of Ga concentrations were not accurate enough (±20%) to extract its segregation coefficient. The distribution plotted using k_{Ga}=0.0086 remains however within the error margins of the SIMS measurements. This good agreement between theory and measured segregation coefficients is very important since the calculation of the Ga concentration to be added is based on those.

Due to its very low segregation coefficient in Si, Ga is heterogeneously distributed along the ingot height. As can be observed (**Fig.4**), Ga concentration is very low in the first solidified fraction of the ingot compared to its initial concentration in the melt. The incorporated Ga concentration then increases towards the end of crystallization. This allows counterbalancing the increase of P concentration towards the end of crystal growth without resulting in a too high net doping in the first

solidified part.

In order to evaluate the net doping vertical distribution in the ingot, we executed room temperature Hall effect measurements on samples taken at various ingot heights. The difficulty in interpreting Hall effect measurements arises from the fact that the measured Hall carrier density p_H differs from the true carrier density p by a factor close to unity (**Eq.2**), called the Hall factor r_H, which depends on the main scattering mechanism.

$$p = r_H \cdot p_H \qquad \textbf{Eq. 2}$$

The r_H dependence on the concentration of doping impurities and on temperature has already been studied for uncompensated p-type Si [14,15]. Although no data was found in the literature for r_H in highly compensated Si, recent results suggest that it is only weakly dependent on the compensation level [16]. In this work, r_H is thus assumed to be equal to 0.7 at room temperature for all samples, as predicted for uncompensated p-type Si with similar doping impurities concentration.

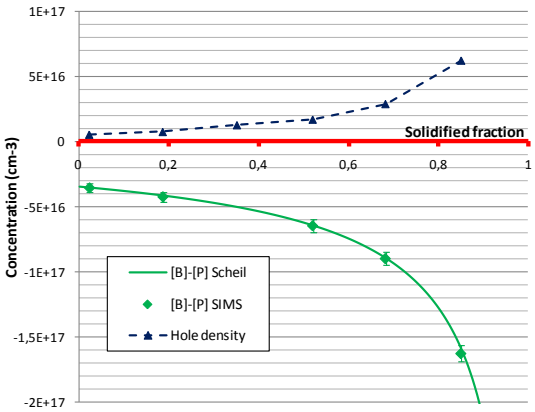

Figure 5 Hole density distribution along the ingot height compared to the net doping [B]-[P] that would be obtained without Ga co-doping.

The measured hole density is plotted against the solidified fraction in Fig.3 together with the net doping [B]-[P] measured by SIMS that would be obtained without Ga addition. Again, it is shown that without Ga co-doping, the ingot would be fully n-type since the net doping [B]-[P] is negative along the full ingot height. In addition, one can observe that while the net doping [B]-[P] without Ga co-doping varies in a wide range, the equilibrium hole density with Ga co-doping remains below 6×10^{16}cm^{-3} over 85% of the ingot height. This thus demonstrates that Ga can be used as a way to monitor the compensation level in order to obtain a relatively low net doping along the full ingot height while crystallizing ingot using B and P compensated Si.

3.3 Carrier mobility and lifetime

The hole mobility is calculated from the Hall effect measurements previously mentioned. Again, in all samples we take r_H as equal to 0.7 to deduce the hole drift mobility from the measured Hall mobility. This mobility is compared in Fig. 4 to that calculated with Arora's model [17]. No significant difference is observed between the measured carrier mobility and Arora's model in the last solidified ingot fraction which contains the largest amounts of Ga. This indicates that Ga does not affect carrier transportation in significantly different manner than boron. In the first solidified fraction of the ingot, measured mobilities are significantly below those predicted by the model. These discrepancies were already observed by Veirman et al. [16] in highly compensated Si suggesting the existence of a specific compensation-related scattering mechanism limiting the carrier mobility. In the ingot studied in this work, the compensation level $C_l=(N_A+N_D)/p$ is the highest in the first solidified fraction (C_l=20 at f_s=0.02 compared to C_l= 6.6 at f_S = 0.85) which might explain the disagreement with Arora's model in this region.

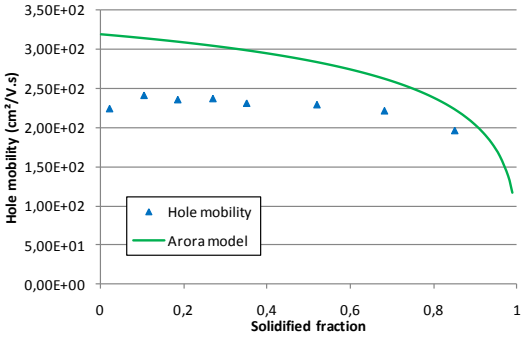

Figure 6 Hole drift mobility deduced from measured Hall mobility considering r_H=0.7 and compared to Arora's model.

QSSPC lifetime measurements were carried out to evaluate the impact of doping impurities on the electrical quality of Si. Results (Fig.7) show that relatively high lifetimes are obtained after recovery in the major part of the ingot, considering the quality of the Si feedstock. A decrease in the minority carrier lifetime is observed as the solidified fraction increases which can be attributed, as proposed by Dubois et al. [3] to the increase in the majority carrier density and thus of the recombination strength of the defects energy states in the band gap of the Si. The very low carrier lifetimes measured in the bottom part of the ingot may also be due to the appearance of high densities of dislocations in this part of the ingot, as observed during crystal growth with the disappearance of the four facets on the edge of the ingot, representative of the dislocation-free <100> oriented mono-crystal.

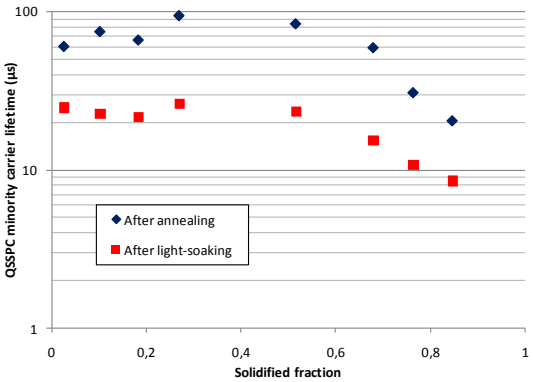

Figure 7 Evolution of the minority carrier lifetime measured for each sample at the injection level $\Delta n=0.1\times p$.

A significant degradation of minority carrier lifetime is observed after light-soaking suggesting the activation of the well-known boron and oxygen related complex [18]. Further studies have to be carried out to determine whether the presence of Ga has an impact on the formation of such complex.

4 CONCLUSION

Thanks to Ga co-doping we control the net doping along the ingot height during crystallization of B and P compensated Si. This method may thus be used to increase the B and P concentration limits allowed in UMG-Si to produce high quality solar cells. The axial distribution of doping species was studied and showed good agreement with theory. Carrier mobility and lifetime measured along ingot height suggest that the full ingot is appropriate for the realisation of good performance solar cells. Significant LID was however measured in these wafers. Solar cells are currently undergoing processing to assess the photovoltaic potential of this material.

5 REFERENCES

[1] R. Einhaus, J. Kraiem, F. Cocco, Y. Caratini, D. Bernou, D. Sarti, G. Rey, R. Monna, C. Trassy, J. Degoulange, Y. Delannoy, S. Martinuzzi, I. Périchaud, M. C. Record, P. Rivat, *Proc. 21st ECPVSEC, Dresden, Germany, 2006*

[2] J. Kraiem, B. Drevet, F. Cocco, N. Enjalbert, S. Dubois, D. Camel, D. Grosset-Bourbange, *Proc. 35th IEEE Photovoltaic Specialists Conference, Hawaii, USA, 2010*

[3] S. Dubois, N. Enjalbert, and J. P. Garandet, *Appl. Phys. Lett. 93, 032114 (2008)*

[4] D. Macdonald, F. Rougieux, A. Cuevas, B. Lim, J. Schmidt, M. Di Sabatino and L. J. Geerligs, *J. Appl. Phys. 105, 093704 (2009)*

[5] E. Enebakk, A. K. Søiland, J. T. Håkedal, R. Tronstad, in: *3rd Intenational Workshop on Crystalline Silicon Solar Cells, SINTEF/NTNU, Trondheim, Norway, 2009*

[6] J. Kraiem, R. Einhaus and H. Lauvray, World patent WO/2009/130409

[7] J. Kraiem, R. Einhaus and H. Lauvray, *Proc. 34th IEEE Photovoltaic Specialists Conference, Philadelphia, USA, 2009.*

[8] D. Macdonald and A. Cuevas in: *19th Workshop on Crystalline Silicon Solar Cells & Modules: Materials and Processes, NREL, Vail, Colorado, 2009.*

[9] M. Forster, E. Fourmond, R. Einhaus, H. Lauvray, J. Kraiem, M. Lemiti, Accepted for publication in *physica status solidi c*

[10] F. Lissalde et al. *Proceedings of the 22nd European PVSEC, Milano 2007, pp. 948 – 951.*

[11] J. Kraiem et al. *Proceedings of the 23rd European PVSEC, Valencia 2008, pp. 1071 – 1074.*

[12] J.-F. Lelièvre, E. Fourmond, A. Kaminsky, O. Palais, D. Ballutaud, M. Lemiti, *Solar Energy Materials & Solar Cells 93, 1281 (2009)*

[13] F. A. Trumbore, *Bell Syst. Tech. J. 39, 205 (1960)*

[14] J. F. Lin, L. C. Linares and K. W. Teng, *Solid-State Electron. 24, 827 (1981)*

[15] F. Szmulovicz, *Phys. Rev. B. 34, 4031 (1986)*

[16] J. Veirman, S. Dubois, N. Enjalbert, J. P. Garandet, D. R. Heslinga and M. Lemiti, *Solid-State Electron. 54, 671 (2010)*

[17] N.D. Arora, J.R. Hauser, D.J. Roulston, *IEEE Trans. Electron Devices, 29, 292, (1982)*

[18] K. Bothe, J. Schmidt, *J. Appl. Phys. 99, 013701 (2006)*